

MEASUREMENT OF NANOMETER ELECTRON BEAM SIZES WITH LASER INTERFERENCE USING IPBSM

Jacqueline Yan, Sachio Komamiya, Masahiro Oroku, Taikan Suehara, Yohei Yamaguchi,
Takashi Yamanaka, University of Tokyo, Tokyo, Japan
Yoshio Kamiya, ICEPP, University of Tokyo, Tokyo, Japan
Sakae Araki, Toshiyuki Okugi, Toshiaki Tauchi, Nobuhiro Terunuma, Junji Urakawa, KEK,
Ibaraki, Japan

Abstract

An e- beam size monitor, called the “Shintake Monitor” (or “IPBSM”), is installed at ATF2’s virtual interaction point (“IP”). It plays a crucial role in achieving ATF2’s Goal 1 of focusing the vertical e- beam size (σ_y^*) down to a design value of 37 nm, using an ingenious technique of colliding the e- beam against a target of laser interference fringes. σ_y^* is derived from the modulation depth of the resulting Compton signal photons measured by a downstream γ detector. IPBSM is the only existing device capable of measuring σ_y^* as small as 20 nm with better than 10% resolution, and can accommodate a wide range of σ_y^* up to a few μm by switching between laser crossing angles $\theta = 174^\circ$, 30° , and $2^\circ - 8^\circ$ according to beam tuning status.

The effects of several major hardware upgrades have been confirmed during beam time, such as through suppressed signal jitters, improved resolution and stable measurements of σ_y^* down to about 150 nm by Feb 2012. The aims of the extensive 2012 summer reform implemented upon the laser optics are higher reliability and reproducibility in alignment. Our goal for the autumn 2012 run is to stably measure $\sigma_y^* < 50$ nm. This paper describes the system’s design, role in beam tuning, and various efforts to further improve its performance.

INTRODUCTION

The International Linear Collider (ILC) holds great potential for detection and detailed research of new physics beyond the Standard Model. Clean e-e+ collisions enable observations of the most fundamental processes free of synchrotron radiation loss. However ILC faces stringent demands for luminosity, expressed here as:

$$L = \frac{n_b N^2 f_{\text{rep}}}{4\pi\sigma_x \sigma_y} H_D \quad (1)$$

n_b : no. of bunches, N : bunch population,
 f_{rep} : repetition rate, H_D : disruption parameter.

It is apparent from the Gaussian beam cross section in the denominator that beam focusing is crucial for achieving high luminosity. The design IP beam sizes for ILC are $(\sigma_x^*, \sigma_y^*) = (640, 5.7)$ nm[1]. At the Accelerator Test Facility 2 (ATF2), a FFS test facility for ILC located in KEK, “Goal 1” is to verify the “Local Chromaticity Correction” scheme by demonstrating focusing of σ_y^* to 37 nm, the design size energy-scaled down from ILC[2]. “Goal 2” is to nm precision beam trajectory stabilization under such a small σ_y^* . IPBSM, installed at ATF2’s

virtual IP, is the only existing device capable of measuring σ_y^* as small as 20 nm. Its outcomes are indispensable for Goal 1, and thus for realization of ILC.



Figure 1: Location of Shintake Monitor in the ATF(2) beamline [3,7].

Measurement Scheme of IPBSM

Figure 2 shows the schematic layout of IPBSM, which consists of laser optics, a γ detector, and DAQ electronics[5]. The pulsed laser beam is split into two paths by a half mirror, then made to cross to form interference fringes at their focal points matched to IP. The phase between the paths, controlled by a piezoelectric stage, is scanned relative to the e- beam traversing the fringes perpendicularly. A downstream γ detector measures the modulation depth (M) of the resulting Compton scattered photon signal at each phase. M is large for focused beams, and small for dispersed beams (Fig. 3).

Laser fringe intensity is expressed using intensity of magnetic field (\mathbf{B}), averaged over time as:

$$\overline{B_x^2 + B_y^2} = B^2(1 + \cos\theta \cos 2k_y y) \quad (2)$$

x and y are coordinates perpendicular to e- beam. $k_y = k \sin(\theta/2)$ (θ : laser crossing angle, λ : laser wavelength) is wave number component normal to fringes. Assuming Gaussian distribution, N , number of Compton photons, is related to beam centre y_0 and σ_y^* as[4].

$$N \propto \int_{-\infty}^{\infty} \frac{1}{\sqrt{2\pi}\sigma_y} \exp\left(-\frac{(y-y_0)^2}{2\sigma_y^2}\right) (B_x^2 + B_y^2) dy \quad (3)$$

$$\Rightarrow N = \frac{N_0}{2} \left\{ 1 + \cos(2k_y y_0) \cos\theta \exp\left(-2(k_y \sigma_y)^2\right) \right\}$$

M , interpreted as ratio of amplitude to average, is calculated in Eq. (4) from N_+ and N_- , max. and min., respectively, of signal intensity. Figure 3 relates M and σ_y^* , calculated as in Eq. (5). Here, measurable range is determined by the laser fringe pitch “ d ” (Table 1)[5, 7].

$$M = \frac{N_+ - N_-}{N_+ + N_-} = |\cos(\theta)| \exp(-2(k_y \sigma_y)^2) \quad (4)$$

$$\sigma_y = \frac{d}{2\pi} \sqrt{2 \ln \left(\frac{|\cos(\theta)|}{M} \right)} \quad d = \frac{\pi}{k_y} = \frac{\lambda}{2 \sin(\theta/2)} \quad (5)$$

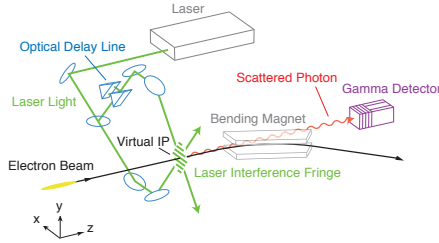


Figure 2: Schematic layout of IPBSM[6].

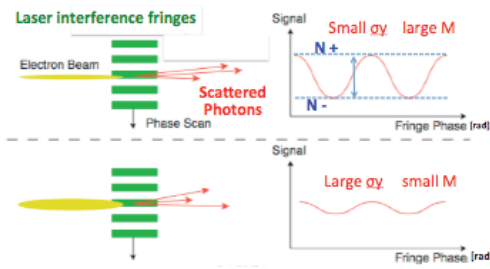


Figure 3: Relationship between beam size and modulation depth.

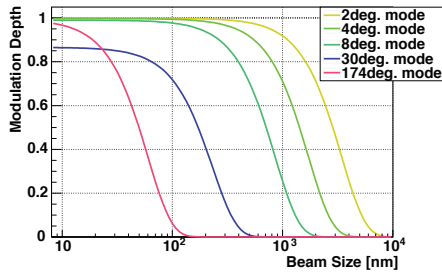


Figure 4: Plot of modulation depth vs σ_y^* for each θ mode[6].

Table 1: Observable σ_y^* Vary with Fringe Pitch, Which Depends on θ

Crossing angle θ	174 deg	30 deg	8 deg	2 deg
Fringe pitch d	266 nm	1.028 μm	3.81 μm	15.2 μm
Measurable σ_y^*	20- 110 nm	80- 400 nm	360 nm-1.4 μm	1.2 ~ 6 μm

Comparison with IPBSM at FFTB

Shintake Monitor had first been put into practical usage at Final Focus Test Beam (FFTB) at SLAC, where it had succeeded in measuring $\sigma_y^* \sim 70$ nm with 10% resolution, whereas the design size was 40 nm[2,4].

Table 2 shows the major changes in IPBSM related parameters from FFTB to ATF2. In order to produce narrower fringe pitches to measure the smaller ATF2 σ_y^* , λ was halved by SHG from 1064 nm to 532 nm. The

measurable range was widened to encompass σ_y^* as large as several μm by adding continuously adjustable lower θ modes. A new multi-layer CsI(Tl) γ detector separates signal from BG by taking advantage of their clearly distinct energy spectrum due to the much lower beam energy at ATF2. Instead of the FFTB method of shifting the e- beam using steering magnets, at ATF2, tuning of the lower energy e- beam is maintained effective by scanning laser fringes relative to a fixed e- beam.

Owing to these accommodations, IPBSM at ATF2 is capable of similar resolution as FFTB despite challenges such as much lower beam energy, single photon energy, and repetition rate.

Table 2: Typical e- Beam and IPBSM Parameters: ATF2 vs FFTB [2, 4]

	FFTB	ATF2
Beam energy	46.6 GeV	1.28 GeV
1 photon energy	8.6 GeV	15 MeV
rep. rate	30 Hz	1.56 Hz (3 Hz)
e- / bunch	1×10^{10}	1×10^{10}
Bunch length	3 ps	16 ps
(σ_x^*, σ_y^*) at IP	(900, 60) nm	(2200, 37) nm
Laser wavelength	1064 nm	532 nm (SHG)
Range for σ_y^*	40-720 nm	20 nm-6 μm

Overall Layout of the Laser Optics

The laser source, located in a separate laser hut, uses SHG to create 8 ns (FWHM) Nd:YAG Q-switch laser pulses at $\lambda = 532$ nm with an intense peak power of 164 MW. The laser beam is delivered to IP through a 30 m transport line containing intermediate mirrors and expanders/reducers to adjust spot size and divergence.

After emerging onto the upright “vertical table” at IP, the laser beam is divided by a 50% beam splitter into upper and lower paths which are focused tightly by lenses at IP, where they cross to form interference fringes. The e- beam, also focused to a waist at IP, is collided against these fringes, then dumped safely. Meanwhile Compton signal photons proceed into the downstream γ detector.

Depending on the targeted σ_y^* , “mode switching” between $\theta = 174^\circ$, 30° , and $2^\circ - 8^\circ$ (continuously adjustable) is carried out by remote control of mover stages carrying mirror actuators. Meanwhile, weakened laser light is admitted to diagnostic devices e.g. PSDs, PIN-PDs, and CCD cameras for real-time monitoring of alignment, phase, timing, intensity and profile.

PERFORMANCE

IPBSM and Beam Tuning

Measurement by IPBSM commences after σ_y^* has been tuned below about 3 μm , confirmable by wire scanners. Multi-knob tuning of beam trajectory may affect shower energy deposit into the γ detector, thus degrading resolution. We check deviation of signal photon path by sliding in a movable collimator with a 10 mm ϕ center, and if necessary adjust beam orbit or collimation.

M detection requires precise laser position alignment, and a sufficiently focused laser waist to be matched strictly to IP. First, laser spots are overlapped with e-beam spot within $O(10\ \mu\text{m})$ precision on a screen monitor inserted into IP. Following this is the finer “laserwire scan”, where one laser path at a time is scanned transverse to e-beam using mirror actuators, and laser position is set to the peak of the resulting Gaussian Compton signal. Similarly, a “z-scan” resolves longitudinal offset to achieve the sharpest fringe contrast i.e. deepest modulation. Laser Q-switch timing is synchronized with beam timing using precise digital delay modules. Stable operation requires suppression of timing jitter $< 1\ \text{ns}$.

After completing all spatial and temporal alignments, IPBSM continuously feeds the σ_y^* it measures using interference scans back to the beam focusing process.

Expectations

IPBSM is capable of measuring σ_y^* from 20 nm to a few μm with resolution better than 10%, assuming 90 bunch measurements, $S/N = 3.5$ and 50 % bunch-by-bunch BG fluctuation[6]. The expected accuracy for measuring the design beam size is

$$37 \pm 2(\text{stat.})_{+4}^{-0}(\text{syst.})\ \text{nm} \quad (6)$$

The following subsections describe (a) statistical errors, the source of signal jitters that hinder M detection, and (b) systematic errors, which cast a lower measurable limit for σ_y^* by smearing fringe contrast, thus under-evaluating M.

Statistical Errors

It becomes more challenging to suppress statistical errors below 10% as σ_y^* is focused down very small, since the stringent beam optics implemented to realize sudden focusing may generate extra BG and lower S/N. Measurement precision of a smaller σ_y^* is impacted more heavily by Compton signal fluctuations [6,7]. The major sources are described as follows[6,7].

Detector Resolution: Resolution of the detector, which separates signal from BG using their distinct shower development, may become degraded when energy spectrum is altered due to (1) Change over time in gain or light collectivity (2) unexpected BG levels and sources (3) photon energy loss due to collision with collimators (4) fluctuation in beam size or trajectory.

Laser Timing and Intensity: Because 8 ns (FWHM) laser pulses interact with much shorter 16 ps e-beam pulses, even a few ns change in laser timing will trigger pulse-to-pulse inconsistency in the laser power felt by the beam during its passage. Fluctuations in laser timing and total power are monitored using TDC and PD, respectively, and are measured during typical operation is measured to be 1 - 2%, with precision better than 1 %.

ICT Monitor Resolution: By normalizing signal energy by beam current measured using an “integrated current transformer (ICT) monitor”, the impact from beam current jitter is suppressed down to the monitor resolution, measured to be about 2.5 - 5%.

Systematic Errors

Systematic errors are interpreted using “modulation reduction factors” C_i ($i = 1, 2, \dots$). These smear laser fringe contrast and reduce M_{meas} from its theoretical value as $M_{\text{meas}} = C_\alpha C_\beta \dots M_{\text{ideal}}$ i.e. over-evaluate $\sigma_{y,\text{meas}}$ as $\sigma_{y,\text{meas}}^2 = \sigma_y^2 + |\Sigma \ln C_i|/2k_y^2$. It is crucial to estimate the effect from these laser and/or beam related factors and correct $\sigma_{y,\text{meas}}$ accordingly. Certain factors affect only 174 deg measurement of $\sigma_y^* < 50\ \text{nm}$ (see Table 3[6,7]).

Laser position and profile at IP: Laser crossing is generally well aligned to e-beam center at IP within $0.1 \cdot \sigma_{\text{laser}}$ using mirror actuators with $< 50\ \text{nm}$ resolution. Fine readjustment is conducted in between scans while monitoring jitters or drift. Meanwhile, profile imbalance between the two laser paths, due to lens misalignment, cast significant local bias on fringe intensity.

Relative position jitter: Fluctuation in relative position between beam and laser smears the M curve. By the time we measure $\sigma_y^* < 50\ \text{nm}$, beam position jitter, likely from magnet vibrations or unstable extraction from damping ring, will be monitored by $O(\text{nm})$ resolution “IPBPMs”

Fringe tilt: A tilt between the e-beam and the transverse plane on which laser fringes form can be observed from the relative offset between the two misaligned laser spots upon the final focal lenses after laser paths have been initially overlapped with beam position on a screen at IP.

Spherical wavefronts: If the e-beam collides at a point offset from laser waist, it would feel “distorted” fringes, due to the finite curvature of the spherical Gaussian wavefronts. Movers attached to the 174 deg final lenses, is expected to scan and align laser focal point to IP within $100\ \mu\text{m}$ precision when measuring the smallest σ_y^* .

Change of beam size within fringe: Measurement of an ultra focused e-beam, whose waist is tuned exactly to IP, is vulnerable to fluctuation in σ_y^* inside the finite longitudinal length of laser fringes. Alignment precision must be reinforced for the heavily impacted 174° mode.

Table 3: Upper Limits of Each M Reduction Factor Predicted for Measuring the Design $\sigma_y^* = 37\ \text{nm}$ at ATF2. Assumed here are nominal laser and ATF2 beam parameters, as well as implementation of specific correction functions for the sensitive 174 deg mode used in this case [6]

Modulation reduction factor	37 nm at 174 deg
Total power imbalance	$> 99.8\ \%$
Relative position jitter	$> 98.0\ \%$
Fringe tilt	$> 97.2\ \%$ (tilt $< 1\ \text{mrad}$)
Alignment (t, z)	($> 99.6\ \%$, $> 99.1\ \%$)
Spatial coherence	$> 99.9\ \%$
Spherical wavefronts	$> 99.7\ \%$
Beam size growth within fringe	$> 99.7\ \%$

Major Systematic Errors in Recent Beam Time

Table 4 summarizes M reduction factors analysed using recent measurements of σ_y^* near 500 nm. These error sources were assessed through the 2012 summer upgrade.

Here, one of the most dominant bias factors is profile imbalance between upper and lower laser paths. This can be inferred from the difference in peak energy and sigma (or σ_{laser}) in Compton signal of a pair of laserwire scans.

Another major bias factor is the tilt of laser fringes relative to e- beam. The alignment precision confirmable with eyes after constructing laser paths at IP is about a few mm, corresponding to a tilt of 5 – 20 mrad. Assuming (according to recent status) precision of 3 mm, and IP $\sigma_{\text{laser}} \sim \sigma_x^* \sim 10\mu\text{m}$, this corresponds to a maximum C_{tilt} of 99 % and 83% for 8° and 30° modes, respectively. Assuming design IP σ_{laser} and σ_x^* for 174° mode, suppression of tilt to 1 mrad would improve C_{tilt} to better than 97%, or 1-2 nm in σ_y^* blow-up.

Table 4: Upper limits of Dominant M Reduction Factors for Measuring $\sigma_y^* \sim 500$ nm at 4 deg mode, Estimated using Data from June, 2012

Modulation reduction factor	O(500) nm at 4 deg
Profile imbalance (t, z)	(> 94%, > 89 %)
Relative position jitter	> 95 %
fringe tilt (t, z)	> 95% (tilt < 20 mrad)
Alignment (t, z)	(> 95%, > 99 %)
Polarization	> 98%

BEAM TIME STATUS OF IPBSM

Status in 2010 - 2011

In spring of 2010, due to tentative tuning issues, a special “ $10 \times \beta_y^*$ ” beam optics had been implemented. Though this limited the smallest feasible σ_y^* , it enabled exceptionally high S/N, under which IPBSM measured $\sigma_y^* = 300 \pm 30$ (stat.) $^{+0}_{-30}$ (syst.) nm [6] at 8 deg mode.

In autumn 2010, β_y^* was restored to the nominal 0.1 mm, after which IPBSM measured σ_y^* averaging at 280 ± 90 nm (stat.) at 5.96 deg[6,7]. After this laser optics was immediately switched to commission the 30 deg mode in pursuit of smaller sizes. However M-reconstruction was interrupted by unexpectedly large signal jitters, then by the Great Eastern Japan Earthquake on March 11, 2011. While recovering the IPBSM system alongside rest of ATF, we investigated signal jitter sources and upgraded hardware accordingly. One of major suspects was a significant rise in BG levels, likely due to return of nominal β_y^* optics. This lowered S/N to below 0.5, which degraded detector precision. The long post-IP bending magnet was discovered to be a major bremsstrahlung source. An “intermediate collimator” was installed there, and its effectiveness was verified during the following beam run. Instabilities in trajectory and profile for both e-beam and laser may also have caused large jitters.

We re-commissioned the interference mode for the first time after the earthquake by detecting M at 2° mode under $10 \times \beta_y^*$ optics to measure σ_y^* tuned down to 2.5 – 3 μm . Due to certain issues in beam tuning, such as having to experiment with several sets of (β_x, β_y^*), σ_y^* was tuned to only $\sim 1 \mu\text{m}$ by the end of 2011. However IPBSM demonstrated good resolution in continuously

measuring σ_y^* at 2 - 8° modes. A series of consecutive scans at 5° marked the best status for this run, as $\sigma_y^* = 1058 \pm 23$ (stat.) nm[7]. Meaningful data were accumulated for study of systematic errors and detector resolution. More efficient scan software and display monitors were introduced into the ATF2 control system.

Status in 2012

Beam focusing resumed in early 2012. On Feb 17, we achieved full commissioning of 30 deg mode under $10 \times \beta_y^*$ optics, followed by stable measurement of σ_y^* around 150 nm under $3 \times \beta_y^*$ optics. The best status came from 10 consecutive stable scans which averaged at $M = 0.56 \pm 0.02$ (stat.), $\sigma_y^* = 166.2 \pm 6.7$ (stat.) nm. Figure 5 shows one of these interference scans.

From there, we took advantage of the favorable laser conditions to commence commissioning of the 174 deg mode. At this point σ_y^* has not been sufficiently focused, as β_y^* optics wasn't at nominal. Low S/N and drifts in beam condition made it even more difficult to reproduce such slight M patterns. Thus time was spent in performing various check-ups of hardware and scan methods.

A large part of beam tests was dedicated to optimizing schemes for mode switching, optics setup, and multi-knob tuning. At the lower 2-8 deg modes, we measured large M of 0.8-0.9 i.e. clear fringe contrast, and used these to investigate systematic errors. This provided us with important directions for the 2012 summer upgrade.

Summer Upgrade of 2012

Systematic errors concerning recent beam times are largely due to misalignment of optical components or of the laser beam itself. In 2012 summer, the vertical table laser optics was reformed extensively. The primary aims are higher stability and reproducibility, crucial for fulfilling ATF2 Goal 1. The new layout will also accommodate certain upgrades for Goal 2 planned for early 2013, e.g. installation of a new IP chamber with three IPBPMs. The major upgrades points are as follows.

Firstly, reference lines were precisely redefined on new base plates to guide the travelling laser path, and ensure ideal setup of optical elements. Positioning of final lenses is then strictly checked using CW alignment laser and transparent targets. The focal scan system was introduced for every θ modes by adding movers to all lenses.

Consistency in laser path is particularly important during θ mode switching, as part of σ_y^* focusing process. Angle selection used to be executed by two sets of rotating stages carrying mirrors, shared by all modes. Because these mirrors are also responsible for overlapping laser with e- beam at IP, it is difficult to maintain laser path consistency when switching in between modes to accommodate beam tuning. Therefore, we replaced the rotators with a more reliable combination of mirror on a small linear mover. With one set for each θ mode, this enables independent mirror adjustments.

More effective alignment is expected to alleviate multiple issues such as fringe tilt, non-ideal laser crossing,

offset injection into lenses, and profile imbalance due to difference in focal points between upper and lower paths. Path length difference due to the delay line for fringe phase control inserted into the upper path, is treated by adding a drift space created by image flopping mirrors.

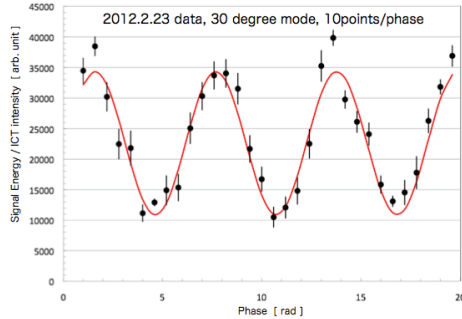


Figure 5: One of the smallest σ_{meas}^* measured at 30° mode. $M = 0.51 \pm 0.02$ (stat.), $\sigma_y^* = 168.5 \pm 6.2$ (stat.) nm (Feb 23, 2012, $10 \times \beta_x^*$, $3 \times \beta_y^*$). Data is plotted as average of ten events at each phase, then χ^2 fitted.

Stabilization of the Laser Optics

Stabilization and careful maintenance of the environment-sensitive laser system is of utmost importance to successful operation. We regularly analyse data collected from temperature sensors strung all around the laser optics. The transport line and its mirror boxes received insulation and anti-vibration reinforcements.

To maintain laser position stable over long operation hours, “Beamlok”, a piezoelectric feedback device was added to the laser cavity, and demonstrates satisfactory performance. Duo-lateral PSDs are installed at several locations to monitor laser position drift and jitters. To confirm compatibility for the upcoming beam run, each PSD and readout DAQ electronics have been individually recalibrated and tested for linearity and signal cross-talk.

Laser oscillation is maintained stable by regular inspections, tuning and exchange of laser cavity mirrors, seeder and flash lamps. These also relaxed laser beam divergence, improved pointing stability at IP, and significantly improved laser profile, which contributed to measurements of clear fringe contrast at lower θ modes.

SUMMARY AND FUTURE GOALS

PBSM is on its way to measuring ATF2’s design σ_y^* while serving as a vital beam tuning tool. At present we have achieved stable measurements of $\sigma_y^* > 150$ nm. Hardware upgrades have been carried out to further suppress systematic errors. Particularly important is the reform of 2012 summer, aimed at improving laser path reproducibility and alignment precision. In preparation for start-up of the ATF2 dedicate runs on Oct.15, we are currently undergoing a series of beam-off tests, such as confirming component positioning precision and optimizing laser spot size and divergence. The effects from the upgrade will be further verified during beam time. We expect to operate under significantly improved precision and stability, and fully commission 174 deg mode i.e. consistently measure $\sigma_y^* < 100$ nm before year end. This demands favorable conditions for both IPBSM laser optics and beam tuning.

After achieving ATF’s goals, the next step is to upgrade IPBSM for utilization as the nm resolution beam size monitor necessary for initial commissioning of the ILC beamline. This demands major modification of laser optics and γ detector to accommodate the higher beam energy, smaller design σ_y^* , and multi-bunch operation at ILC. Although ATF2 is a scaled down prototype, the technologies verified there are directly applicable to ILC. R&D of IPBSM is indeed valuable for realization of ILC-like future Tev scale linear colliders.

REFERENCES

- [1] SB2009 Proposal Document, Rel.1.1, 2009
- [2] B.I. Grishanov et al., ATF2 Collaboration, ATF2 Proposal, KEK Report 2005-2
- [3] T. Shintake, “Measurement of Small Electron-Beam Spots”, Annu. Rev. Nucl. Part. Sci. 1999, 49:125-62.
- [4] P.G.Tenebaum, “Expanded Studies of Linear Collider Final Focus Studies at the Final Focus Test Beam”, SLAC-Report-95-475 (1995).
- [5] T. Suehara: “A nanometer beam size monitor for ATF2” in Nuclear Instruments and Methods in Physics Research A 616 (2010) 1–8
- [6] Y. Yamaguchi, Master thesis at Graduate School of Science, The University of Tokyo (2010)
- [7] J. Yan, Master thesis at Graduate School of Science, The University of Tokyo (2011)